

Monitoring forest health by remote sensing of canopy chlorophyll: first results from a pilot project in Norway

S. Solberg^{a,*}, H. Lange^a, L. Aurdal^b, R. Solberg^b and E. Næsset^c

^a Norwegian Forest Research Institute, Høgskoleveien 8, 1432 Ås, Norway – (svein.solberg, holger.lange)@skogforsk.no

^b Norwegian Computing Centre, Gaustadalléen 23, Post Office Box 114, Blindern, N-0314 Oslo, Norway – (lars.aurdal, rune.solberg)@nr.no

^c Norwegian University of Life Sciences, Dep. of Ecology and Natural Resource Management, P.O.Box 5003, 1432 Ås, Norway – erik.naesset@umb.no

Keywords: remote sensing, forest health, canopy, tree crown modelling, chlorophyll, SPOT, laser scanning

Abstract - Variation in canopy chlorophyll mass per area is a well-suited candidate for tracking temporal changes in forest health. In the current project, we try to apply remote sensing techniques for measuring this. Within a 6 km² forest test area dominated by Norway spruce (*Picea abies*) we have data from three spatial levels: ground, airborne and satellites. On ground we have data on LAI and chlorophyll concentrations from 16 sample plots. The airborne level, comprising LiDAR and hyperspectral data, is used for modelling of LAI and chlorophyll concentrations, and for up-scaling to the entire area. We try to model LAI using LiDAR, and chlorophyll concentrations using the hyperspectral data. Up-scaled data for LAI are correlated to SPOT satellite data. If it turns out that up-scaled estimates are correlated to satellite data, this might form a basis for developing a new forest health monitoring system in Norway and elsewhere.

1. INTRODUCTION

On the global scale forests are threatened by population growth and human activities, including deforestation, air pollution and climate change. There is a need for quantitative information on forest health, and how it varies in space and time. Important here is the need for a quantitative and general health variable integrating across diagnoses, because a global climate change may be manifested by a wide range of different damage types. Remote sensing might now provide useful tools for forest health monitoring. Remote sensing has already demonstrated its ability to provide forest health-relevant data, such as Leaf Area Index (LAI) and leaf loss (Brandtberg 2003; Lefsky et al. 1999; Schaepman et al. 2004), chlorophyll (Malenovsky 2002, Zarco-Tejada et al. 2004), foliar nutrients (Martin & Aber 1997), and identification of trees having root diseases (Leckie et al. 2004). In the current project we try to develop methods where the basic idea is that variation in forest canopy chlorophyll per unit ground area is a suitable measure of variation in forest health, and that this quantity can be estimated from remote sensing data, where LiDAR data provide estimates on LAI and airborne hyperspectral data provide chlorophyll concentration estimates via spectral signatures.

These two variables correspond to the traditional, ground based forest health variables defoliation and discolouration. Forest health monitoring has been run by the European forest monitoring programme UN-ECE/ICP-Forests since 1986, with annual health assessments of 320,000 trees throughout Europe (Anon. 2002). Remote sensing techniques have the advantage compared to traditional, ground based forest monitoring, that they are objective and have full area coverage.

The aim of this paper is to describe preliminary results from a project where we try to develop a method for monitoring of forest health by remote sensing. If this is successful, it might form the basis for a routine monitoring of forest health in Norway by remote sensing.

2. MATERIALS AND METHODS

2.1 Study area

The area for this study is located near Oslo, in south-eastern Norway (59° 50'N, 11° 02' E, 190–370 m a.s.l.). The size of the area is 6 km², comprising mainly Norway spruce (*Picea abies* L. Karst.) and some Scots pine (*Pinus sylvestris* L.). A large part of the area consists of old forest stands only. This area is a forest reserve, where no clear-cuttings have been executed since 1940 and it is considered as a primeval forest, being partly multi-layered. Most of the data were collected during summer 2003. Field work was carried out in July. Satellite data were acquired in August, whereas airborne hyperspectral data were acquired in June 2004.

2.2 Sample plot inventory

We subjectively selected 16 spruce sites for sample plots, being in the four age-classes, II=young plantations, III=thinning-phase forest, IV-V=older forest, having corresponding tree heights in the plots being around 0.5-6; 7-14; 15-20; and 21-35 m, respectively. We used differential GPS/GLONASS for determining plot coordinates in field according to the procedures proposed by Næsset (2001) and demonstrated in a similar project by Næsset (2004). Positions of all trees were obtained by additional measurements of their polar coordinates within the plot. For all trees we recorded diameter at breast height (dbh), defoliation, discolouration, social status, and tree species.

On each plot, four of the non-suppressed trees were systematically selected as sample trees, being the first tree found going clockwise around the plot after each main cardinal direction. On these 64 sample trees, we measured height, crown base, and crown width in four cardinal directions. One branch was sampled from the lower, the middle and the upper parts of the crown (crowns divided in three equally long parts). The branches were stored at below zero temperatures in the field and during transport to the laboratory, and analyzed for chlorophyll concentrations in the foliage.

For 11 of the sample plots, we measured optical Leaf Area Index using a LiCor LAI-2000 plant canopy analyzer. For each circle, five values were obtained by measuring at the center and 3 m away from the center in each of the four cardinal directions. The forest area was classified into stands, with tree species and age class given for each stand. This was done as part of a operational forest inventory by a commercial company in Norway (Prevista).

2.3 Airborne laser scanner data

Laser data were acquired on October 10, 2003, by a Hughes 500 helicopter carrying the ALTM 1233 laser scanning system produced by Optech, Canada. The leaf conditions were in an intermediate state, i.e. the deciduous trees were still foliferous at the time of the flight. The average flying altitude was approximately 600 m. Twenty-one flightlines were flown with an overlap between adjacent lines of about 20 %. The laser-scanning covered almost entirely the 6 km² forest area (Fig. 1). GPS and inertial navigation system data were logged continuously to provide geometric correction and geo-referencing.

First and last returns were recorded. The last return data were used to model the terrain surface. A triangulated irregular network (TIN) was generated from the planimetric coordinates and corresponding height values of the individual terrain ground points retained in the last pulse dataset. All first and last return observations (points) were spatially registered to the TIN according to their coordinates, and the relative height of each point was computed as the difference between their height values and the terrain surface height.

2.4 Airborne hyperspectral data

Hyperspectral data were acquired on June 30, 2004, by a Cessna 172 airplane carrying the ASI (Airborne Spectral Imager) developed by Norsk Elektro Optikk AS, Norway (Anon. 2004). The average flying altitude was 900-1200 m above the ground. Four flightlines were flown, covering all the 16 sample plots, however, the area coverage was only ca 20 % of the forest area. GPS and inertial navigation system data were logged continuously to provide geometric correction and geo-referencing of the images. The data set was radiometrically calibrated to obtain radiance.

The ASI instrument is a pushbroom scanner consisting of two camera modules, covering the VNIR (400-1000 nm) and SWIR (1000-1700 nm) spectral regions. Only the VNIR module was flown during this campaign. This module covers the spectral range with 160 bands, yielding a spectral sampling interval of 3.7 nm. The across-track field of view is 17° distributed among 1600 spatial pixels, giving a FOV pr pixel of ~0.14mrad (pixel size ~14cm at 1000m altitude).

2.5 Satellite data

We have one SPOT quarter-scene acquired on August 17, 2003. The image is a level 3 SPOT image. This data set has a spatial resolution of 10x10 m, with four spectral bands: green, red, NIR and SWIR. Also, we have one Hyperion scene acquired on August 3, 2003. This image has a 30x30 m spatial resolution, and comprises 242 spectral bands in the wavelength range 355-2577 nm. The images were geo-referenced and radiometrically corrected.

2.6 LAI and remote sensing data

We estimated LAI from LiDAR data assuming that laser pulses penetrate the canopy layer in a similar way as solar radiation. Light interception in the canopy layer follows Lambert-Beer's law, where relative log-transformed light intensity values decrease linearly with increasing LAI. Recalculating the LiDAR data according to this provided LiDAR interception values over the entire area. LiDAR interception values were averaged for each of the 1000 m² sample plots, and correlated to the ground based LAI measurements. From this we derived a model for LAI estimation based on the LiDAR data. We also correlated ground based LAI values to SPOT NDVI.

2.7 Segmentation of trees in DSM using LiDAR data

In order to assign pixels from the airborne hyperspectral data set uniquely to sample trees, the crown outlines were modelled using the LiDAR point cloud. The main steps in the tree segmentation algorithm were filtering of the laser data to retain only the uppermost LiDAR points; making a digital canopy surface model (DSM) by smoothing these points into a grid; locating local maxima in the DSM as tree top candidates; and applying a watershed algorithm to identify the tree crown outlines for each local maximum. These outlines (polygons) were then linked to the tree numbers from the ground data, based on the stem coordinates of the trees. Hyperspectral pixels were then derived from an overlay of these polygons on the hyperspectral images (Fig. 3).

2.8 Modelling of chlorophyll using hyperspectral data

We selected chlorophyll concentrations measured in the upper part of the tree crowns for correlating with hyperspectral data. In general, green plants have a very specific spectral signature, with low reflectance in visible light, and high reflectance in the near infrared range, i.e. the red-edge effect. We correlated chlorophyll concentrations to spectral variables that reflect this red-edge effect, i.e. so far NDVI. Exploiting the full set of (160) channels available from the hyperspectral images (in contrast to the SPOT images), we calculated wavelength-dependent canopy reflectance (normalized to standardized).

2.9 Up-scaling and relationships to satellite data

We intend to use the empirical models between foliar mass and LiDAR, and between chlorophyll concentrations and hyperspectral data for up-scaling of the ground truth to every pixel in the satellite scenes. It has been shown (Carter and Spiering 2002) that this usually leads to a maximum correlation coefficient of 0.9 and above.

3. RESULTS

The young plots generally contained more and smaller trees compared to the older plots. Some key data are presented in table 1.

Concerning foliar mass or LAI, we have results linking ground measurements to satellite data, using airborne data as link between them. The 11 plots with LAI measurements had LAI values ranging from 0.85 to 5.3. In general the young stands (type II) had values around 1, the slightly older stands (type III) had very variable values ranging from 1 to 5, while the older stands (type IV and V) had values around 3.

Table 1. Mean values for the number of trees pr plot; diameter at breast height (cm); height of sample trees (m); and chlorophyll concentration ($\mu\text{g/g}$ fresh weight) by plot type

| Age class | No trees | dia | height | Chl |
|-----------|----------|-----|--------|------|
| II | 156 | 5 | 4 | 944 |
| III | 203 | 8 | 9 | 1100 |
| IV | 107 | 17 | 23 | 1126 |
| V | 102 | 19 | 28 | 1040 |

The LiDAR interception values were strongly related to the ground based LAI values, $R^2=0.95$. The model was applied to the entire forest area covered by airborne laser scanning. Every 10×10 m square got an estimated LAI value based on the model and the LiDAR data from that square. The squares were put on a regular grid, which matched exactly the position and size of the SPOT satellite pixels.

This, together with SPOT satellite data and forest stand data produced a data set of 46,000 pixels having both LAI estimates and SPOT NDVI, and where the main tree species was Norway spruce (Fig. 1). There was a relationship between the two variables LAI and NDVI. High LAI values and high NDVI values were generally seen in dense or old forests, mostly in lower parts of the terrain, while low values were seen mostly in upper hillsides and hill tops, which are dominated by scattered pine and aspen trees, and on clear cuttings and young stands. However, the match between NDVI and LAI was far from perfect. Some dense stands with young spruce trees had high NDVI values, but low LAI values. A preliminary, non-linear model between LAI and NDVI, following the approach of Roberts et al. (2004), gave a weak but significant relationship ($R^2=0.16$), with a saturation point of ca. 0.8 for NDVI at LAI-values around 4 and higher, when excluding clear-cuttings.

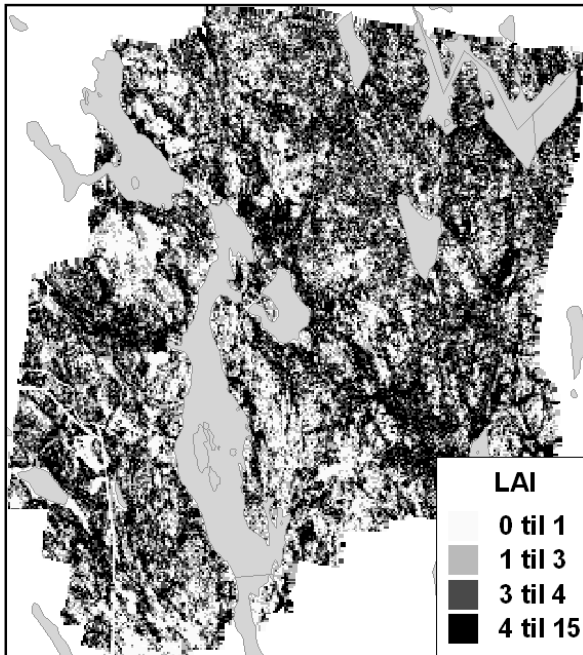


Fig. 1. Map of the forest area showing leaf area index estimated from LiDAR for a 10×10 m grid.

We have also obtained a strong correlation directly between the 11 LAI measurements and SPOT NDVI ($R^2 = 0.85$). We used the average NDVI for 3×3 pixels around each plot. The variance in NDVI between age classes, between replicates within an age class, and within a plot is evident in Fig. 2.

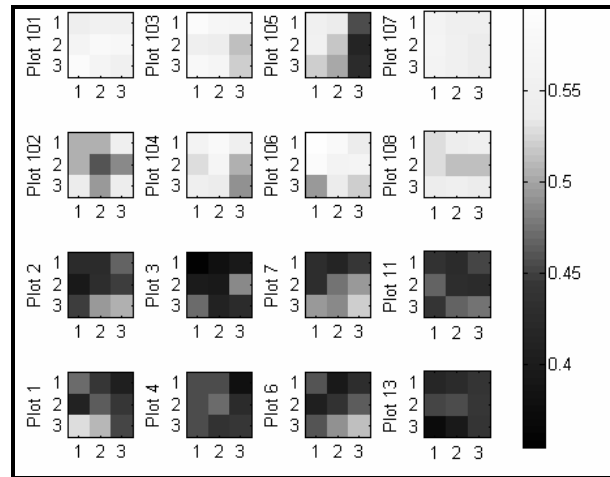


Fig. 2. SPOT based NDVI values for the 16 sample plots, one age class per row (uppermost = young stands, lowermost = old stands) and the four replicates in columns. Each plot is covered by 3×3 pixels.

Concerning modelling of chlorophyll concentrations using hyperspectral data, we are in the beginning of the work only. A first step here is modelling of the outline of single trees, in order to extract pixels from airborne, high-resolution, hyperspectral data. This step is finished and we have started to overlay tree outline polygons on the hyperspectral images (Fig. 3). So far, we have data for 16 of the 64 sample trees.

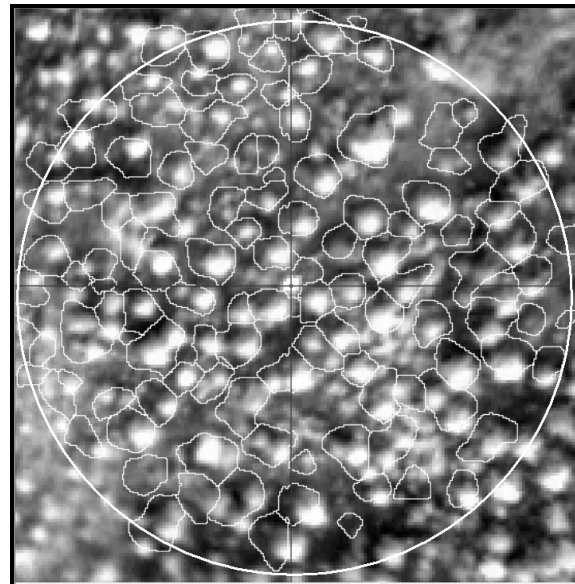


Fig. 3. Tree crowns segmented from LiDAR data, overlaid on hyperspectral image.

The sample trees had very similar hyperspectral signatures, one of which is shown in Fig. 4. Based on the crown delineation, the tree has a crown area of 4.6 m^2 , leading to 116 spectra, which are then averaged.

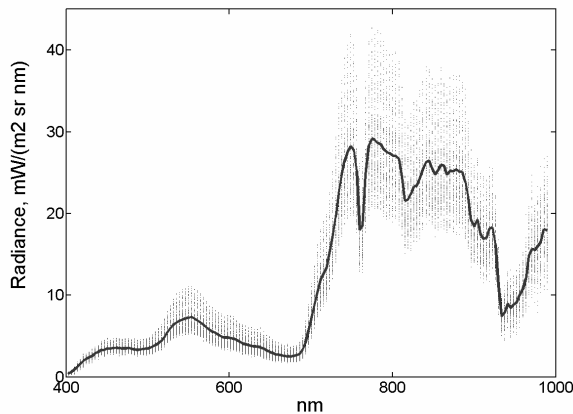


Fig. 4. Spectral signature for one young spruce tree. Spectra for all 116 pixels (dots) and the average (line) are shown.

From the averaged spectra for the 16 sample trees, we calculated an NDVI index by summing channels in accordance with the Landsat TM bands R and IR. Foliage chlorophyll concentrations in the upper canopy were positively, but only weakly ($R^2=0.12$) related to NDVI in the hyper-spectral data.

4. DISCUSSION AND CONCLUSIONS

Airborne LiDAR appears to be a good data type for LAI estimation, and repeated surveys thus have a great potential to track changes in LAI, i.e. changes in defoliation over time. Also, LiDAR data has proven suitable for modelling of individual trees, being necessary for attributing ground based data on single trees to airborne hyperspectral data. These are the major result of the project so far. Concerning relationships between chlorophyll concentrations and hyperspectral data, we have only preliminary results for a fraction of the sample trees. One caveat in our data here, is the one year difference between ground data and hyperspectral data, caused by technical problems. Concerning possible relationships between satellite data and up-scaled estimates of LAI and chlorophyll, more analyses are needed. In conclusion, remote sensing techniques appear to be useful for forest health monitoring, but it is still too early from our project whether a monitoring can be done using satellites or airplanes, and also the role of hyperspectral data is still unclear.

REFERENCES

- Anon. 2002. UN/ECE & EC. / Lorenz, M., Mues, V., Becher, G., Müller-Edzards, Ch., Luyssaert, S., Raitio, H., Fürst, A., Langouche, D. Forest Condition in Europe - 2003 Technical Report, Geneva, Brussels
- Anon. 2004. ASI – Airborne spectral imager. NEO (Norsk Elektro Optikk AS) <http://www.neo.no/asi>
- Brandtberg, T., Warner, T., Landenberger, R. and McGraw, J., 2003. Detection and Analysis of Individual Leaf-off Tree Crowns in Small Footprint, High Sampling Density Lidar Data from the Eastern Deciduous Forest in North America, *Remote Sensing of Environment*, vol. 85, no. 3, pages 290-303.

Carter, G.A., and B.A. Spiering 2002. Optical properties of intact leave for estimating chlorophyll concentration. *J. Environ. Qual.* 31,1424-1432.

Leckie, D.G., Jay, C., Gougeon, F.A., Sturrock, R.N. and Paradine, D. 2004. Detection and assessment of trees with *Phellinus weirii* (laminated root rot) using high resolution multi-spectral imagery. *International Journal of Remote Sensing* 25, 793-818.

Lefsky, M., Cohen, W., Acker, S., Parker, G., Spies, T. and Harding, D. 1999. Lidar Remote Sensing of the Canopy Structure and Biophysical Properties of Douglas-Fir Western Hemlock Forests, *Remote Sensing of Environment*, vol. 70, no. 3, pages 339-361.

Malenovský 2002. Investigation of functional parts and status of Norway spruce crowns using spectral remote sensing information. Thesis Report GIRS 25. Lab of Geo-Inf Science and Rem Sens, Wageningen Univ, pp. 1-74

Martin, M.E. & Aber, J. D. 1997. High spectral resolution remote sensing of forest canopy lignin, nitrogen, and ecosystem processes. *Ecological Applications* 7: 431-443.

Næsset, E. 2001. Effects of differential single- and dual-frequency GPS and GLONASS observations on point accuracy under forest canopies, *Photogramm. Eng. Remote Sensing* 67, 1021-1026.

Næsset, E. 2004. Practical large-scale forest stand inventory using small-footprint airborne scanning laser. *Scand. J. For. Res.*, 19, 164-179.

Roberts, D.A., Ustin, S.L., Ogunjemiyo, S., Greenberg, J., Dobrowski, S.Z., Chen, J. and Hinckley, T.M. 2004. Spectral and Structural Measures of Northwest Forest Vegetation at Leaf to Landscape Scales. *Ecosystems* 7, 545-562.

Schaepman, M.E., Koetz, B., Schaepman-Strub, G., Zimmermann, N.E. & Itten, K.I. 2004. Quantitative retrieval of biogeophysical characteristics using imaging spectroscopy: a mountain forest case study. *Community Ecology*, in press.

Zarco-Tejada, P.J., Miller, J.R., Morales, A., Berjón, A. and Agüera, J. 2004. Hyperspectral indices and model simulation for chlorophyll estimation in open-canopy tree crops. *Remote Sensing of Environment* 90, 463-476.

ACKNOWLEDGEMENTS

Norwegian space agency and Norwegian forest research institute are acknowledged for financing the study. Ivar Baarstad and Trond Løke from Norsk Elektro Optikk AS are acknowledged for recording and georeferencing of hyperspectral images with the ASI sensor.